Desalination and Water Treatment
www.deswater.com

doi: 10.1080/19443994.2015.1074620

57 (2016) 15889–15899
July

Taylor & Francis
Taylor & Francis Group

Fenton process-driven decolorization of Allura Red AC in wastewater using apolaccase-modified or native nanomagnetite immobilized on silica fume

Azize Alayli Gungor[a], Hayrunnisa Nadaroglu[b], Ekrem Kalkan[c,*], Neslihan Celebi[a]

[a]*Department of Chemical Technology, Erzurum Vocational School, Ataturk University, 25240 Erzurum, Turkey, emails: aalayli@atauni.edu.tr (A. Alayli Gungor), nes25@atauni.edu.tr (N. Celebi)*
[b]*Department of Food Technology, Erzurum Vocational School, Ataturk University, 25240 Erzurum, Turkey, email: hnisa25@atauni.edu.tr*
[c]*Oltu Earth Sciences Faculty, Department of Geological Engineering, Ataturk University, 25400 Oltu-Erzurum, Turkey, email: ekalkan@atauni.edu.tr*

Received 10 January 2015; Accepted 13 July 2015

ABSTRACT

Magnetite ($FeO{\cdot}Fe_2O_3$) nanoparticles immobilized on silica fume modified by treatment with apolaccase were used to decolorize, by way of Fenton and Fenton-like processes, Allura Red AC dye present in industrial wastewater. Surface changes to the silica were investigated by scanning electron microscopy, Fourier transform infrared spectroscopy, X-ray diffraction, and energy-dispersive X-ray spectroscopy. The decolorization system's operational parameters: $3 \le pH \le 9$; $20\,^{\circ}C \le Temp. \le 80\,^{\circ}C$; contact time, 0–180 min; initial Allura Red AC concentration, 0–50 mg L^{-1}; and adsorbent concentrations, 0–200 mg L^{-1} were studied to understand their effects on Allura Red AC removal. The optimal parameters values were: pH 5.0; temperature, 30–60°C; decolorization time, 30 min; initial Allura Red AC concentration, 50 mg L^{-1}; and adsorbent concentration: 1 g/L. Under these conditions, immobilized magnetite nanoparticles and their apolaccase-modified counterparts showed decolorization efficiencies of 83.11 and 85.60%, respectively, for the removal of Allura Red AC from industrial wastewater by way of Fenton and Fenton-like processes. These experiments also showed the adsorbent to be reusable, cheap, biocompatible, easy to prepare, non-toxic (magnetite nanoparticles, H_2O_2, and silica fume), and capable of generating Fenton reaction conditions with or without additional treatment with apolaccase. The adsorbent was shown to be useful in the decolorization of toxic dyes from industrial wastewater.

Keywords: Nano-Fenton process; Apolaccase; Allura Red AC; Decolorization; Wastewater

1. Introduction

The food, plastics, tannery, paint, paper, pulp, and fabric industries employ significant quantities of over 10,000 synthetic dyes [1]. Textile dyes alone are produced at a rate of over 0.7 Tg y^{-1} [2]. As a result of the production process, 10–15% (by weight) of dyes are released into wastewater [3]. Waste dyes pose health and environmental dangers, including some which are potential carcinogens. Given their hazardous effects, the decolorization of dyes from wastewater has become an important and attractive approach to minimizing their deleterious effects on health and environment.

*Corresponding author.

Dyes can be categorized in a number of ways, including (i) the material to which they are applied, (ii) their chemical structure (e.g. azo triaryl methane, anthraquinone, heterocyclic dye, and phthalocyanine dyes), and (iii) the method/process of their application (e.g. container, reactive, straight, acidic, dissolved, and cationic) [4].

The use of large quantities of dyeing compounds during the various stages involved in dyeing foods and textiles during their transformation or manufacturing has led to serious environmental contamination issues [5]. Apart from the visual problems associated with colored waste, dyes also powerfully absorb sunlight, thus hindering the photosynthetic activity of water plants and reacting very aggressive throughout the whole environment [6]. Most of the dyes disposed of are non-decomposable by the microflora and direct biological treatment of colored effluent is not effective in terms of decolorization [7]. Therefore, physical and/or chemical management methods have to be used to decolorize or partially degrade the dyes in dye house effluent to make them more susceptible to secondary biological management [8–12].

Allura Red AC is a red azo dye that goes by several names, including: Allura Red, Food Red 17, C.I. 16035, FD&C Red 40, and E129. The IUPAC name is disodium: (5E)-5-[(2-methoxy-5-methyl-4-sulfonatophenyl) hydrazinylidene]-6-oxonaphthalene-2-sulfonate. Its major areas of use are as a color additive in food, drugs, and cosmetics [13]. It is used to color gelatins, puddings, custards, alcoholic and non-alcoholic beverages, sauces, toppings, candy, sugars, frostings, fruits, juices, dairy products, bakery products, jams, jellies, condiments, meat, and poultry. One expects Allura Red AC dye to be mobile in soil as it exists in the environment almost exclusively in anionic form and anions generally do not adsorb strongly to soils containing organic carbon and clay than their neutral counterparts [14].

Methods such as coagulation/flocculation, activated carbon adsorption, and reverse osmosis can only transfer the contaminants from one phase to another [15]. Therefore, a great deal of attention has been paid to the development of water treatment techniques that lead to complete destruction of the dye molecules. Because of the high oxidative power of the hydroxyl radical, numerous processes based on the group of compounds of this type have been categorized under the term of progressive oxidation processes (AOPs). These processes have been used in the reducing both harmless and refractory organic, as well as inorganic, contaminants found in water or wastewater. The most often used AOPs entail heterogeneous photocatalytic oxidation [16–20], ozonation joined with hydrogen peroxide (H_2O_2), ultraviolet (UV) light, or both [21,22], H_2O_2/UV, as well as Fenton and photo-Fenton reagents [23].

Extensively studied and well-described Fenton technology is as a remarkable alternative for the management of industrial wastewater bearing non-biodegradable organic contaminants [24]. Heterogeneous Fenton and Fenton-like processes have recently received a great deal of attention. In heterogeneous Fenton reactions, iron salts are adsorbed on the surface of different materials serve as supported catalysts when placed in an appropriate aqueous environment. The reduction–oxidation reactions between Fe (II) and Fe(III) take place in the presence of hydrogen peroxide which promotes the formation of reactive components such as (·OH) and hydroperoxyl (·OOH) radicals (Eq. (1) [25]. The radicals produced by the breakdown of hydrogen peroxide can then oxidize organic compounds.

$$Fe^{2+} + H_2O_2 \rightarrow Fe^{3+} + {}^{\cdot}OH + {}^{\cdot}OOH \quad (1)$$

The area of active iron ion is present at both the reagent area and loose liquid stage. Consequently, the Fe(III)/Fe(II) complex generated on the support material can react with H_2O_2, thus permitting iron ions to join in the Fenton catalytic cycle Eqs. 2(a)–2(d) [26–28].

$$Fe^{2+} + H_2O_2 \leftrightarrow Fe-OOH^{2+} + H^+ \quad (2a)$$

$$Fe-OOH^{2+} \rightarrow HO_2^* + Fe^{2+} \quad (2b)$$

$$HO_2^* + Fe^{2+} \rightarrow Fe^{3+} + H_2O^- \quad (2c)$$

$$HO_2^* + Fe^{3+} \rightarrow Fe^{2+} + O_2 + H^+ \quad (2d)$$

Laccase (benzenediol: oxygen oxidoreductase, EC 1.10.3.2) represents a small portion of a wide group of enzymes called polyphenol oxidases. Having copper atoms in their catalytic area, these are often termed multicopper oxidases [29]. Laccase-driven catalysis arises with reduction of oxygen to water accompanied by the oxidation of substrate. Laccases are oxidases that oxidize polyphenols, methoxy-substituted phenols, aromatic diamines, and a variety of other compounds [30]. These enzymes are used for pulp delignification, pesticide or insecticide degradation [31], organic synthesis, waste detoxification, textile dye transformation, food technological uses, and biosensor and analytical applications [32,33].

The present work investigated the decolorization of Allura Red AC by heterogeneous Fenton and Fenton-like processes using immobilized nanomagnetite on silica fume, either in native form or modified with an apolaccase catalyst. The effects of different initial immobilized magnetite nanoparticle concentrations, initial pH, initial contact time, initial temperature, and initial Allura Red AC concentration on the decolorization efficiency (DE) of the process were investigated and are discussed.

2. Materials and methods

2.1. Chemical and reagents

DEAE-Sephadex, ammonium sulfate, ABTS [2,2′ azino-bis (3-ethylbenzylthiazoline-sulphanic acid)], Na_2HPO_4, CH_3COONa, dipicolinic acid, Allura Red AC (Fig. 1), magnetic nanoparticles of Fe_3O_4 (iron I, II oxide) [34], silica fume, and hydrogen peroxide (30%, w/w) were purchased from Sigma–Aldrich. The pH of the solution was adjusted using 0.1 M HCl or 0.1 M NaOH. All the chemicals used were of analytical grade, and were employed without any further purification. Distilled water was used throughout.

2.2. Adsorbent

Silica fume, also known as microsilica, is a byproduct of the reduction of high-purity quartz with coal in electric furnaces in the production of silicon and ferrosilicon alloys. It is also collected as a byproduct in the production of other silicon alloys such as ferrochromium, ferromanganese, ferromagnesian, and calcium silicon. Silica fume was obtained from a ferrochromate factory in Antalya, Turkey [35].

2.3. Adsorbent preparation

The silica fume was washed to neutrality with distilled water. The suspension was wet sieved through a 200 mesh screen. The solid fraction was washed five times with distilled water following a sequence of mixing, settling, and decanting. The last suspension was filtered, and the residual solid was then dried at 105°C, ground in a mortar, and sieved through a 200 mesh sieve. The chemical and physical properties of the resultant material are summarized in Table 1. A sample of silica fume (1 g) was shaken with 10 mL, 108 CFU mL^{-1} *M. extorquens* solution for approximately 1 h, and the separated particles were then stored [35].

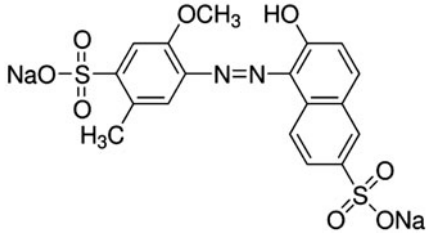

Fig. 1. Chemical structure of Allura Red AC.

Table 1
General characteristics of magnetic nanoparticles Fe_3O_4 and Allura Red AC

Nanoparticles	Nanomagnetite	Allura Red AC
Chemical formula	Fe_3O_4	$C_{18}H_{14}N_2Na_2O_8S_2$
Molar mass (g mol^{-1})	231.53	496.421899
Surface area (m^2 g^{-1})	>60	–
Particle size (nm)	50–100	–
Compound ID	–	6,093,299
λ_{max} (nm)	–	405

2.4. Preparation of magnetite nanoparticles immobilized on silica fume surface

To generate immobilized nanoparticles, 0.03 M Fe_3O_4, in the form of magnetic nanoparticles, was prepared the material in 100 mL of deionized water, to which 25-g silica fume were added. The resultant slurry was mixed for 24 h using a stirrer (500 rpm, 25°C). The slurry was centrifuged at 5,000 rpm for 20 min. The pellet was washed three times with distilled water to remove residual Fe_3O_4. The resultant wet paste was dried in an oven at 40°C for 72 h. The immobilized surface was grinned before use in experiments.

2.5. Purification of laccase enzyme

Lactarius volemus (Fr.) Fr. (1838) were picked in April–May near the city of Hasankale in Turkey's eastern province of Erzurum. The species was recognized by a botanist and specimens were held at −40°C to avoid spoilage. *L. volemus* (10 g) was powdered in liquid N_2, then mixed uniformly with 50 ml of 1 M KCl in a blender, and centrifuged at 5,000 ×*g* for 60 min. The enzyme, present in the supernatant, followed the methods of [36], which included ammonium sulfate precipitation anion exchange chromatography and gel filtration chromatography (Table 2). The purification folds were calculated to be A 146.13-fold purification was achieved (Table 2). The protein content of chromatographic eluates was measured (Beckman Coulter

Table 2
The purification process of laccase from Russulaceae (*L. volemus*)

Enzyme fraction	Volume (mL)	Activity (EU mL^{-1})	Total activity		Protein (mg mL^{-1})	Specific activity (EU mg^{-1})	Purification Fold
			EU	%			
Crude extract	100	121.5 ± 1.31	1.22×10^4	100	195.2 ± 0.32	0.62	–
$(NH_4)_2SO_4$	95	93.2 ± 0.11	8.85×10^3	72.5	45.1 ± 1.25	2.07	3.34
DEAE-Sephadex	40	72.1 ± 1.11	2.88×10^3	32.5	6.1 ± 2.31	11.82	19.1
Sephacryl S 200	30	65.2 ± 0.33	1.96×10^3	68.1	0.72 ± 1.10	90.6	146.13

Du 730 Life Science UV/vis) spectrophotometrically at 280 nm and by the Bradford method [37].

The ABTS reagent was used as a substrate in the spectrophotometric determination of laccase activity. One activity unit (U) represented the amount of enzyme that oxidized 1 μmol of ABTS min^{-1} and enzyme activity was expressed in U l^{-1} [38,39].

2.6. Preparation of apolaccase enzyme

Laccase (100 mg) was dissolved in 5 mL of 0.2 M phosphate buffer (pH 7.0) containing 0.075 M dipicolinic acid. The solution, which was placed into a dialysis sack, dialyzed in 1 L of the same buffer for 5 h. Subsequently, it was dialyzed for 18 h against deionized water, including 5–6 changes. Following these, the solution was dialyzed for 5 h against 0.01 M acetate buffer (pH 5.0), which also served in activity measurement. At this point, almost 100% pure apoenzyme was obtained [40].

2.7. Surface characterization of Fe_3O_4 immobilized on silica fume

The chemical and mineralogical composition of Fe_3O_4 immobilized on silica fume samples was determined by scanning electron microscopy and various spectral analyses. A scanning electron microscope (SEM; Metek, Apollo prime, Active area 10 mm^2, Microscope inspect S50, SE detector R580) was used to examine the surface of native adsorbent and metal-loaded adsorbent, at a 5,000-fold magnification.

Before SEM examinations, sample surfaces were coated with a thin layer (20 nm) of gold to obtain a conductive surface and to avoid electrostatic charging during examination. The same procedure was also used for the energy dispersive X-ray (EDX) spectra analysis in order to determine the elemental composition of the powdered Fe_3O_4 immobilized silica fume.

In addition, the Fourier transform infrared spectroscopy (FTIR) analyses were carried out to identify functional groups and molecular structure in the Fe_3O_4-immobilized silica fume and enzyme-modified Fe_3O_4-immobilized silica fume. FTIR spectra were recorded on a Mattson 1000 FTIR spectrometer. The spectrum of the adsorbent was measured within the range of 4,000–400 cm^{-1} wave numbers.

The XRD pattern of adsorbent was determined by XRD (Rigaku D-Max 2000) and analyzed with CuKα (λ = 0.154 nm) radiation with 2θ, 5°–100° (with a step size of 0.1) (Fig. 6).

2.8. Decolorization study

All decolorization experiments were made in a 100-mL stoppered Erlenmeyer flasks containing Allura Red AC (50 mg L^{-1}) and 100-mg Fe_3O_4 immobilized on silica fume. The pH was adjusted to the desired value using either 0.1 M NaOH or 0.1 M HCl. The reactions were initiated by adding 0–10% w/w H_2O_2 solution to the flasks. The flasks were placed in a shaker (200 rpm) at the room temperature and sample aliquots taken out of the flasks periodically, using a micropipette. The reaction mixture samples were centrifuged at 5,000 rpm for 10 min. The supernatant was filtered through 0.45-nm filters. The concentration of Allura Red AC was measured spectrophotometrically (Beckman Coulter Du 730 Life Science UV/vis) at 545 nm.

The effect of the quantity of magnetite nanoparticles immobilized on silica fume was studied by varying the surface material concentration between 12.5 and 200 mg. Also, the activity of the catalyst to decolorize Allura Red AC was tested under different reaction parameters: $3 \le pH \le 9$, $20\,^{\circ}C \le T^{\circ} \le 80\,^{\circ}C$, and initial concentration of Allura Red AC from 3.25 to 50 ppm.

The DE of Allura Red AC was defined as:

$$DE(\%) = 100 \times \frac{[\text{Allura Red AC}]_0 - [\text{Allura Red AC}]_t}{[\text{Allura Red AC}]_0} \quad (3)$$

where [Allura Red AC]$_0$ is the initial concentration of Allura Red AC (mg L^{-1}), and [Allura Red AC]$_t$ is the concentration of Allura Red AC (mg L^{-1}), at reaction time, t (min).

3. Results and discussion

3.1. Surface characteristics of Fe_3O_4 immobilized on silica fume

The SEM is useful for determining the particle shape, porosity, and appropriate size distribution of the adsorbent [33]. The SEM images of native adsorbents and Allura Red AC dye-loaded adsorbents were recorded and shown in Fig. 2. In the SEM micrograph of Fig. 2(a), the bright spots show the rough and porous surface of the adsorbent, which is one of the factors increasing adsorption capacity. The loaded SEM images show the adsorption of Allura Red AC dye on the adsorbent. In Fig. 2(b) and (c), depicting the surfaces of particles after adsorption, it is clearly seen that the caves, pores, and surfaces of adsorbent were covered by dye and consequently the surface has become smooth. It is evident that upon adsorbing the dye, the adsorbent structure has changed [41].

The EDX measurements were recorded for qualitative analysis of the element constitution of the adsorbents and the EDX spectra of native adsorbent and Allura Red AC dye-loaded adsorbent were illustrated in the Fig. 3(a–c). The Allura Red AC dye ions were adsorbed onto the silica fume-nanomagnetite and silica fume-nanomagnetite-apolaccase adsorbents. It is shown from EDX spectra that after dye adsorption, element concentrations increased in the Allura Red AC dye-loaded adsorbents Fig. 3.

In addition, the FTIR analyses were carried out to identify functional groups and molecular structure. Silica fume-nanomagnetite, silica fume-nanomagnetite-Allura Red AC, and silica fume-nanomagnetite-Allura Red AC-apolaccase surface structure are shown in Fig. 4. The structure of silica was compared with nanomagnetite-immobilized silica and enzyme-modified nanomagnetite-immobilized silica (Fig. 4(a–c)). Silica bonds and the bonds of the structure of the vibrational bands—Si–O (563 cm^{-1}), silanol –OH bend (794 cm^{-1}), the asymmetric Si–O–Si stretching, tetrahedral form SiO_4 (1,129.4 cm^{-1}), molecular water bending –OH (1,630.34 cm^{-1}), and adsorbed water and OH stretch (3,000–3,800 cm^{-1}), respectively—were observed. Especially after doing Fenton reaction completely change the structure of the finger print region, silica-magnetite nanoapolaccase Allura Red AC structure indicates that this reaction was occurred [42].

The XRD patterns of adsorbent and Allura Red AC dye-loaded adsorbents are presented in Fig. 5. The XRD pattern of silica fume-nanomagnetite has sharp and wide peaks. However, these characteristic peaks either disappeared or were weakened in the XRD pattern of Allura Red AC-loaded silica fume-nanomagnetite and silica fume-nanomagnetite-apolaccase. Therefore, crystalline structures of native adsorbents were damaged [43].

3.2. Decolorization study

3.2.1. Optimal dosage of H_2O_2

Currently, we know that the efficiency of the Fenton reaction depends mainly on H_2O_2 concentration. H_2O_2 concentration varied from 1 to 5%. Every time,

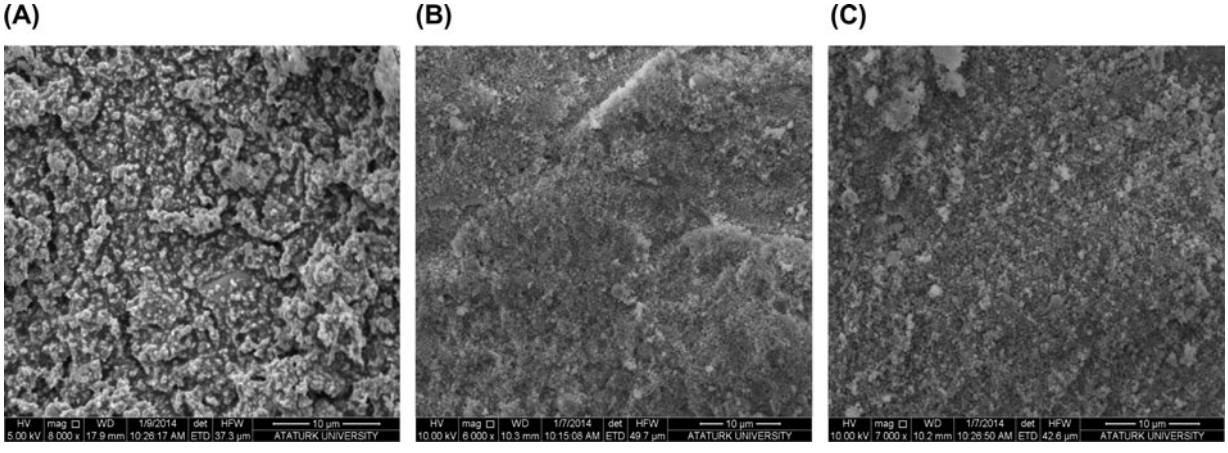

Fig. 2. SEM images of adsorbents (A) Silica fume-nanomagnetite, (B) silica fume-nanomagnetite-Allura Red AC, and (C) silica fume-nanomagnetite-apolaccase-Allura Red AC.

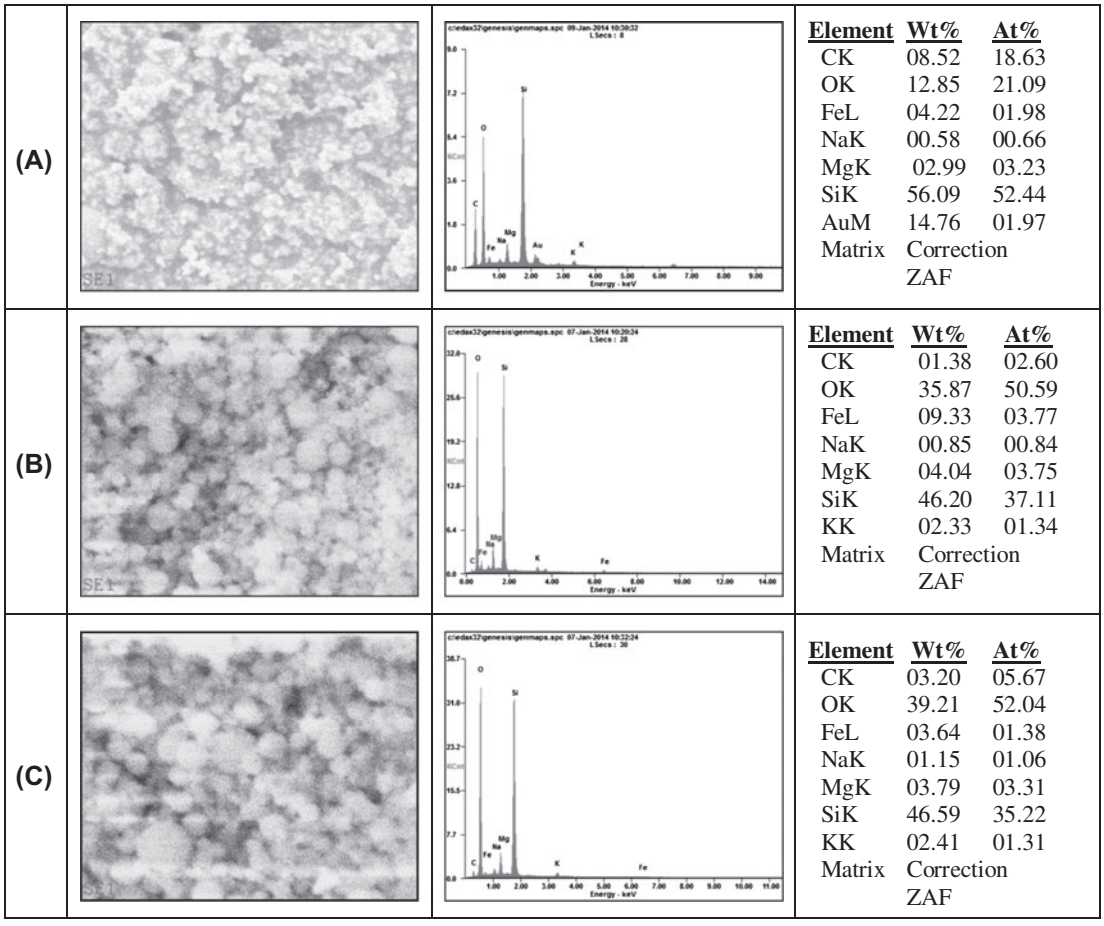

Fig. 3. EDX images of adsorbents (A) Silica fume-nanomagnetite, (B) silica fume-nanomagnetite-Allura Red AC, and (C) silica fume-nanomagnetite-apolaccase-Allura Red AC.

Fenton's reagent was prepared fresh and used in the experiment. All the experiments were carried out with 100-mg apolaccase-modified or native silica fume and other Fenton's reagent. All the reactions were initially carried out at same conditions. The reaction was carried out in a shaker. The reaction mixture was filtered and then the Allura Red AC amount was measured [44]. The DE of Allura Red AC was estimated as described in Fig. 6.

3.2.2. Contact time

A plot of dye removal *vs.* contact time (Fig. 7) shows that Allura Red AC removal increases in over the first 30 min of contact time. Basically, the removal of copper is fast at the beginning and gradually decreases with time until it reaches an equilibrium rate. This is indicated by the fact that the Allura Red AC in the solution decreased rapidly within 15 min and the removal was virtually completed within 30 min of contact time.

3.2.3. Effect of pH

The pH level of the aqueous reaction solution is an important operational parameter in the decolorization process as it affects solubility of the dye, concentration of counter ions on the functional groups of the adsorbent, and the degree of ionization of the adsorbate during the reaction [44]. In other words, the uptake and percentage removal of metals from the aqueous solution are strongly affected by the pH of the solution [45–47]. Showing the removal of Allura Red AC over a pH range of 3–9, Fig. 8 showed pH values in the upper fives to yield the best dye removal.

Lin and Lo was declared the wastewaters containing PVA/Blue-G and PVA/ Black-B, respectively, treated by the Fenton treatment process [48–50]. Both figures clearly show that, as the pH increases above 3, there is a rapid increase in the COD concentration, indicating an optimal pH 3 for the Fenton treatment process.

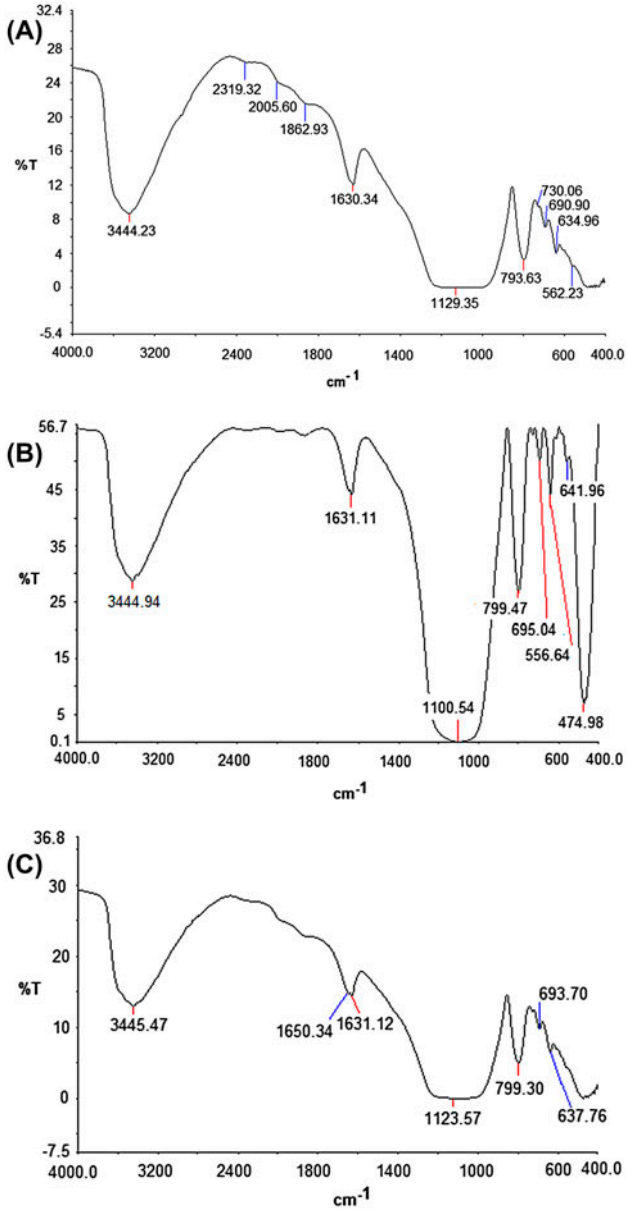

Fig. 4. FTIR images of adsorbents (A) Silica fume-nanomagnetite, (B) Silica fume-nanomagnetite-Allura Red AC, and (C) Silica fume-nanomagnetite-Allura Red AC-apolaccase.

On the other hand, $OH^{\cdot}$ is the oxidizing species involved in the oxidative processes connected with Fenton reaction [51]. Also, a study of the reduction of dissolved iron species by humic acid has suggested that in addition to the $OH^{\cdot}$ radical another oxidant may be involved in the Fenton reactions in the seawaters at neutral pH (7.0–7.5). Other studies suggest that at nanomolar levels of Fe(II), the oxidation of Fe(II) by H_2O_2 in the seawater predominantly involves the $FeOH^{+}$ species at pH 6.0–8.0.

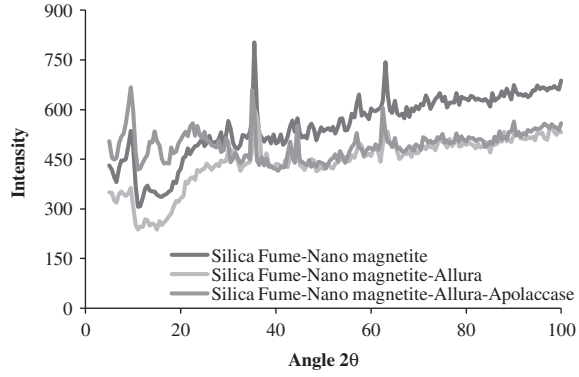

Fig. 5. XRD images of adsorbents.

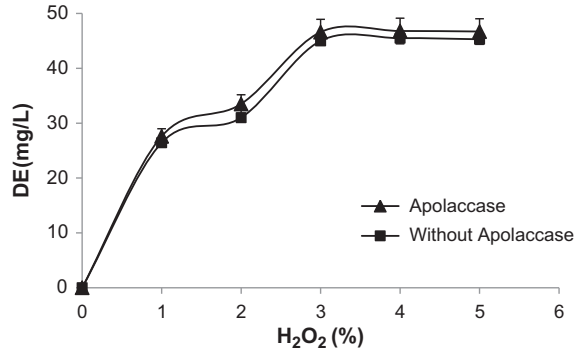

Fig. 6. Optimal dosage of H_2O_2.

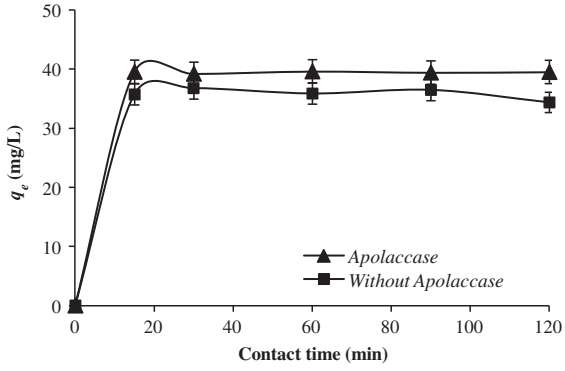

Fig. 7. Effect of contact time on the removal of Allura Red AC by nanomagnetite-immobilized and apolaccase-modified silica fume.

Normally, the Fenton reaction is optimum at 3 pH levels [49–53], but in the present study, the stability of the Fenton reaction at a little bit higher pH 5.0 value was enhanced by immobilization of the magnetite nanoparticles and the apolaccase modification. This

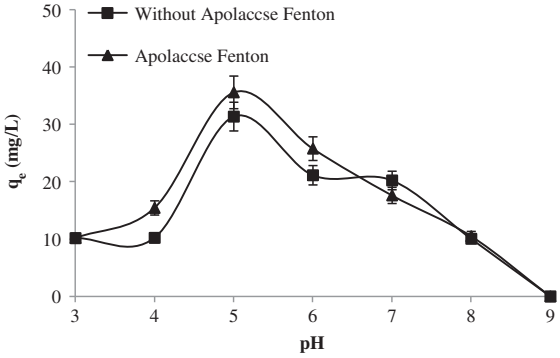

Fig. 8. Effect of pH on the removal of Allura Red AC by nanomagnetite-immobilized and apolaccase-modified silica fume.

dye removal process can be used nearer a neutral pH, thereby decreasing its harmful effects.

3.2.4. Effect of temperature

Temperature is known to have a profound effect on various chemical processes. It affects the adsorption rate by altering molecular interactions and solubility of the adsorbate, Allura Red AC, enzyme, and magnetite nanoparticles [54]. The effect of temperature on the decolorization effect of the Fenton reaction with immobilized magnetite nanoparticles, with or without apolaccase modification is illustrated in Fig. 9. For both native and apolaccase-modified systems, decolorization of Allura Red AC increased in parallel with temperatures from 20 to 30˚C, where it peaked, then declined slightly at the higher temperatures of 40 and 60˚C. The effectiveness of the process at the upper temperatures is advantageous in treating industrial discharge given its generally higher temperatures.

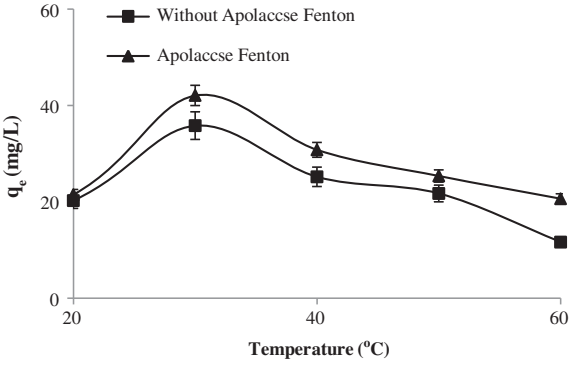

Fig. 9. Effect of temperature on the removal of Allura Red AC by nanomagnetite-immobilized and apolaccase-modified silica fume.

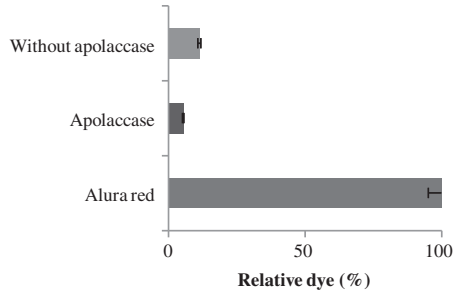

Fig. 10. Decolorization of Allura Red AC-Fenton and apolaccase enzyme-modified Fenton reaction.

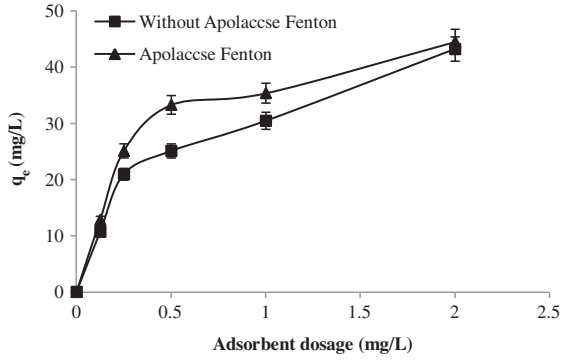

Fig. 11. Effect of adsorbent dosage on the removal of Allura Red AC by nanomagnetite-immobilized and apolaccase-modified silica fume.

3.2.5. Effect of Allura Red AC and adsorbent concentrations

Using Fenton and Fenton-like processes—without and with apolaccase, respectively—81 and 87% Allura Red AC removal rates were achieved (Fig. 10). The

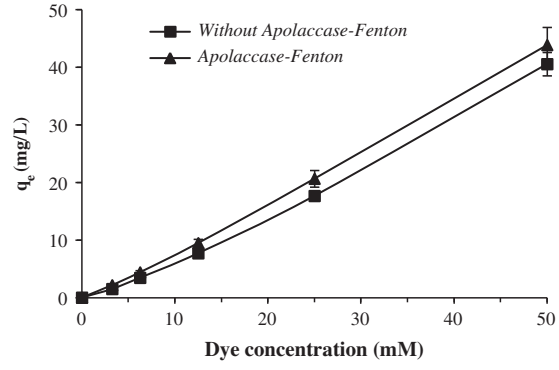

Fig. 12. Effect of dye concentration on the removal by nanomagnetite-immobilized and apolaccase-modified silica fume.

rate of decolorization of Allura Red AC increases substantially with an increase in the concentration of either adsorbent, though the increase in decolorization was slower at adsorbent concentrations exceeding 0.1 g (Fig. 11). The decolorization effect was greater as dye concentration increased (Fig. 12). This optimization of the process conditions (time, pH, temperature, dye, and adsorbent dosages) ensures a high cost and pollutant removal efficiency. So, it was calculated optimum).

4. Conclusions

In our study, using a Fenton and Fenton-like process removal rates of 81 and 87% for the toxic dye Allura Red AC were, respectively, achieved in the absence and presence of apolaccase. Thus, the Fenton and Fenton-like processes were very effective in decolorization. Being inexpensive and widely available, silica fume represents a substrate for magnetite nanoparticles immobilization. The iron has no known toxic effects and is widely available. For this reasons, many industries use metallic iron to remove waste before releasing discharge into the environment. The Fenton process has long been used in the removal of toxic organic substances; however, its use in decolorization of dye from wastewater is relatively new. The reaction rate of the Fenton process increases with temperature; however, the degradation of hydrogen peroxide to water and oxygen was decreased, as was the reaction rate at temperatures above 50˚C. Our research has shown that higher temperatures (e.g. 60˚C vs. room temperature) do not substantially affect the decolorization reaction rate for magnetite nanoparticles immobilized on silica fume in the presence or absence of apolaccase modification. This is an excellent advantage since the fabric dyeing industry released high-temperature wastewater.

Acknowledgments

The SEM, EDX, and FTIR studies presented were carried out in the Faculty of Science, Atatürk University, while the XRD study was carried out in the Faculty of Engineering of the same institution. The authors therefore thank Prof. Dr Umit DEMIR and Prof. Dr Yaşar TOTIK, respectively.

References

[1] R. Baskar, N. Sivarajasekar, Adsorption of Allura Red AC onto activated carbon derived from immature cottonseeds: Isotherm studies and error analysis, Desalin. Water Treat. 52(40–42) 7743–7765.

[2] E. Gurtekin, N. Sekerdag, Color removal from textile wastewater wıth fenton process, J. Eng. Nat. Sci. 26(3) (2008) 216–226.

[3] E. Guivarch, S. Trevin, C. Lahitte, M.A. Oturan, Degradation of azo dyes in water by Electro-Fenton process, Environ. Chem. Lett. 1 (2003) 38–44.

[4] X.R. Xu, H.B. Li, W.H. Wang, J.D. Gu, Degradation of dyes in aqueous solutions by the Fenton process, Chemosphere 57 (2004) 595–600.

[5] D. Georgiou, P. Melidis, A. Aivasidis, K. Gimouhopoulos, Degradation of azo-reactive dyes by ultraviolet radiation in the presence of hydrogen peroxide, Dyes Pigm. 52 (2002) 69–78.

[6] W.G. Kuo, Decolorizing dye wastewater with Fenton's reagent, Water Res. 26 (1992) 881–886.

[7] A. Uygur, E. Kok, Decolourisation treatment of azo dye waste waters including dichlorotriazinyl reactive groups by using advanced oxidation method, J.S.D.C. 115 (1999) 350–354.

[8] M.M. Tatli, G. Aktas, M. Kosecik, A. Yilmaz, Treatment of typhoid fever in children with a flexible-duration of ceftriaxone, compared with 14-day treatment with chloramphenicol, Int. J. Antimicrob. Agents 21 (2003) 350–353.

[9] I.M. Banat, P. Nigam, D. Singh, R. Marchant, Microbial decolorization of textile-dyecontaining effluents: A review, Bioresour. Technol. 58 (1996) 217–227.

[10] O. Kocaer, U. Alkan, Alternatives of treatment of wastewater including textyl dyestuff. University of Ataturk, J. Fac. Eng. Archit. 7(1) (2002) 47–55.

[11] F. Midik, Reaktif sarı 145 azo boyar maddesinin ve 2,4 Diklorofenoksiasetik Asit Pestisitinin Yüksüz Nano Demir, Fenton ve Foto-Fenton Prosesleri ile Karşılaştırmalı Giderilmesi (Comparıson of Degradatıon Actıvıtıes of Azodye Reactıve Yellow 145 and Pestıcıde 2,4-Dıchlorophenoxyacetıc Acıd by Nanoscale Zero Valent Iron, Fenton and Photo-Fenton Process), Masters Thesis, University of Cukurova, Institute of Science, Department of Chemistry, (2011), p. 89.

[12] H. Hassan, B.H. Hameed, Decolorization of acid red 1 by heterogeneous fenton like reaction using fe-ball clay catalyst, International Conference on Environmental Since and Engineering Ipcbee Iacsit Press, Singapore, Vol. 8 (2011).

[13] M.J. O'Neil, The Merck Index—An Encyclopedia of Chemicals, Drugs, and Biologicals, Merck and Co., Inc., Whitehouse Station, NJ, 2006, pp. 22–23.

[14] W.J. Doucette, Handbook of Property Estimation Methods for Chemicals, R.S. Boethling, D. Mackay (Eds.), Lewis Publ., Boca Raton, FL, (2000) 141–188.

[15] F. Torrades, J. García-Montaño, J.A. Antonio García-Hortal, X. Domènech, J. Peral, Decolorization and mineralization of commercial reactive dyes under solar light assisted photo-Fenton conditions, Sol. Energy 77 (2004) 573–581.

[16] M.R. Hoffmann, S.T. Martin, W. Choi, D.W. Bahnemann, Environmental applications of semiconductor photocatalysis, Chem. Rev. 95 (1995) 69–96.

[17] M. Perez, F. Torrades, J.A. Garcia-Hortal, X. Domenech, J. Peral, Removal of organic contaminants in paper pulp treatment effluents by TiO_2 photocatalyzed oxidation, J. Photochem. Photobiol., A Chem. 109 (1997) 281–286.

[18] I. Arslan, I.A. Balcioglu, Advanced oxidation of raw and biotreated textile industry wastewater with O_3, H_2O_2/UV-C and their sequential application, J. Chem. Technol. Biotechnol. 76 (2001) 53–60.
[19] C. Lizama, M.C. Yeber, J. Freer, J. Baeza, H.D. Mansilla, Reactive dyes decolouration by TiO_2 photo-assisted catalysis, Water Sci. Technol. 44 (2001) 197–203.
[20] C.M. So, M.Y. Cheng, J.C. Yu, P.K. Wong, Degradation of azo dye Procion Red MX-5B by photocatalytic oxidation, Chemosphere 46 (2002) 905–912.
[21] I.A. Alaton, I.A. Balcioglu, D.W. Bahnemann, Advanced oxidation of a reactive dyebath effluent: comparison of O_3, H_2O_2/UV-C and TiO_2/UV—A processes, Water Res. 36(5) (2002) 1143–1154.
[22] I. Arslan, I. Balcioglu, Degradation of Remazol Black B dye and its simulated dyebath wastewater by advanced oxidation processes in heterogeneous and homogeneous media, Color. Technol. 117 (2001) 38.
[23] S.K.A. Solmaz, A. Birgul, G.E. Ustun, T. Yonar, Colour and COD removal from textile effluent by coagulation and advanced oxidation processes, Color. Technol. 122 (2006) 102–109.
[24] J. Deng, J. Jiang, Y. Zhang, X. Lin, C. Du, Y. Xiong, $FeVO_4$ as a highly active heterogeneous Fenton-like catalyst towards the degradation of Orange II, Appl. Catal., B Environ. 84 (2008) 468–473.
[25] N.K. Daud, B.H. Hameed, Decolorization of acid red 1 by a Fenton-like process using rice husk ash based catalyst, J. Hazard. Mater. 176 (2009) 938–944.
[26] E. Neyens, J. Baeyens, A review of classic Fenton's peroxidation as an advanced oxidation technique, J. Hazard. Mater. 98 (2003) 33–50.
[27] O.S.N. Sum, J. Feng, X. Hu, P.L. Yue, Novel bimetallic catalyst for the photoassisted degradation of acid black 1 over a broad range of pH, Chem. Eng. Sci. 59 (2004) 5269–5276.
[28] J.H. Sun, S.P. Sun, G. Liang, L.P. Qiao, Degradation of azo dye amido black 10B inaqueous solution by fenton oxidation process, Dyes Pigm. 74(3) (2006) 647–652.
[29] M. Alcalde, Laccase: Biological functions, molecular structure and industrial applications, in: J. Polaina, A.P. Maccabe (Eds.), Industrial Enzymes: Structure, Function and Applications, Springer, New York, NY, 2007, pp. 459–474.
[30] P. Baldrian, Fungal laccases—Occurrence and properties, FEMS Microbiol. Rev. 30(2) (2006) 215–242.
[31] S. Riva, Laccases: Blue enzymes for green chemistry, Trends Biotechnol. 24 (2006) 219–226.
[32] A. Zamorani, Enzymatic processing of musts and wines, in C. Cantarelli, G. Lanzarini (Eds.), Biotechnology Applications in Beverage Production, Elsevier Applied Science, New York, NY, 1989, pp. 223–246.
[33] N.M. Mahmoodi, R. Salehi, M. Arami, H. Bahrami, Dye removal from colored textile wastewater using chitosan in binary systems, Desalination 267 (2011) 64–72.
[34] R.B. De Castro, P.T. Foncesa, J.G. Pacheco, J.C.V. Da Silva, E.G.L. Da Silva, M.H.A. Santana, L-Edge inner shell spectroscopy of nanostructured Fe3O4, J. Magn. Magn. Mater. 233(1–2) (2001) 69–73.
[35] H. Nadaroglu, N. Celebi, E. Kalkan, N. Dikbas, The evaluation of affection of *Methylobacterium extorquens* —Modified silica fume for adsorption cadmium(II) ions from aqueous solutions affection, Kafkas Univ Vet Fak Derg 19(3) (2013) 391–397.
[36] H. Nadaroglu, E. Tasgin, Purification and characterization of laccase from *Lactarius volemus* and its application in removal of phenolic compounds from fruit juice, J. Food Agric. Environ. 11(3–4) (2013) 109–114.
[37] M.M. Bradford, A rapid and sensitive method for the quantification of microgram quantities of protein utilizing the principle of protein–dye binding, Anal. Biochem. 72 (1974) 248–258.
[38] M.L. Niku-Paavola, L. Raaska, M. Itävaara, Detection of white-rot fungi by a non-toxic stain, Mycol. Res. 94 (1990) 27–31.
[39] W. He, H.Y. Zhan, X.W. Wang, H. Wu, An improved spectrophotometric procedure for the laccase assay, J. South China Univ. Technol. 31 (2003) 46–50.
[40] N. Demir, O.I. Küfrevioglu, E. Keha, E.B. Bakan, An enzymatic method for zinc determination, Serumbiofactors 4 (1993) 129–132.
[41] G. Vijayakumar, R. Tamilarasan, M. Dharmendirakumar, Adsorption, kinetic, equilibrium and thermodynamic studies on the removal of basic dye Rhodamine-B from aqueous solution by the use of natural adsorbent perlite, J. Mater. Environ. Sci. 3(1) (2012) 157–170.
[42] G.E.A. Swann, S.V. Patwardhan, Application of Fourier Transform Infrared Spectroscopy (FTIR) for assessing biogenic silica sample purity in geochemical analyses and palaeo environmental research, Clim. Past 7 (2011) 65–74.
[43] D. Hu, P. Wang, J. Li, L. Wang, Functionalization of microcrystalline cellulose with N,N-dimethyldodecylamine for the removal of Congo Red Dye from an aqueous solution, Bioresources 9(4) (2014) 5951–5962.
[44] V.P. Bhange, S.P.M.P. William, A. Sharma, J. Gabhane, A.N. Vidya, S.R. Wate, Pretreatment of garden biomass using Fenton's reagent influence of Fe^{2+} and H_2O_2 concentrations on lignosellulose degradation, Environ. Health Sci. Eng. 13(12) (2015) 1–7.
[45] O.S. Amuda, A.A. Giwa, I.A. Bello, Removal of heavy metal from industrial wastewater using modified activated coconut shell carbon, Biochem. Eng. J. 36 (2007) 174–181.
[46] A. Benhammou, A. Yaacoubi, L. Nibou, B. Tanouti, Adsorption of metal ions onto Moroccan stevensite: Kinetic and isotherm studies, J. Colloid Interface Sci. 282 (2005) 320–326.
[47] S.E. Ghazy, A.H. Ragab, Removal of copper from water samples by sorption onto powdered limestone, Indian J. Chem. Technol. 14 (2007) 507–514.
[48] Y.B. Onundi, A.A. Mamun, M.F. Al Khatib, Y.M. Ahmed, Adsorption of copper, nickel and lead ions from synthetic semiconductor industrial wastewater by palm shell activated carbon, Int. J. Environ. Sci. Technol. 7 (2010) 751–758.
[49] W.G. Kuo, Decolorizing dye wastewater with Fenton's reagent, Water Res. 26 (1992) 881–886.

[50] S.H. Lin, C.C. Lo, Fenton process for treatment of desizing wastewater, Water Res. 31 (1997) 2050–2056.
[51] S. Meriç, D. Kaptan, T. Ölmez, Color and COD removal from wastewater containing Reactive Black 5 using Fenton's oxidation process, Chemosphere 54 (2004) 435–441.
[52] K. Barbusiński, Fenton reaction, Controversy concerning the chemistry, Ecol. Chem. Eng. 16(3) (2009) 347–358.
[53] N. Modirshahla, M.A. Behnajady, F. Ghanbary, Decolorization and mineralization of C.I. Acid Yellow 23 by Fenton and photo-Fenton processes, Dyes Pigm. 73 (2007) 305–310.
[54] H. Nadaroğlu, E. Kalkan, N. Çelebi, Removal of copper from aqueous solutions by using micritic limestone, Carpathian J. Earth Environ. Sci. 9(1) (2014) 69–80.